CHAPTER 6
RESULTS AND DISCUSSION ON SMELTING REDUCTION

This chapter deals with the reduction kinetics of iron ore-coal composite pellets in liquid metal bath, dissolution behaviour of single pellet, and bulk dissolution of composite pellets during smelting reduction in an induction furnace. It also presents the results on auxiliary studies such as X-ray diffraction (XRD) and scanning electron microscopic (SEM) examinations as back-up investigations.

6.1 Visual Observation of Dissolution Behaviour of a Single Pellet

The melting of composite pellets was performed in an induction furnace in a 6 kg capacity, alumina / magnesia lined, melting pot. Initial liquid metal bath was created by melting of cast iron. The liquid metal bath was slagged-off prior to the test. Two different techniques were used in these experiments. One consisted of dropping the pellet on the liquid metal bath, allowing it to move freely on the surface of the liquid metal, observing its behaviour and recording the time it takes to dissolve completely. The other technique consisted of immersing the pellet into the liquid metal bath while it was tied with tungsten wire. The other end of the wire was held in hand firmly to forcibly push the pellets deep into the liquid metal bath. In some cases, stainless steel rod was used to push the pellet into the liquid metal bath. Due to their low density, the pellets float on the surface of the melt and tend to move towards the wall of the melting pot. Partially dissolved pellets were taken out and subsequently observed under scanning electron microscope to determine the structural changes occurred during dissolution.

The interaction of the pellet with the liquid metal bath generated a strong agitation. This is due to the evolution of the gases from the pellet and those being produced during the process by chemical reactions as well as electro-magnetic stirring due to induction. The experiments performed using pellets that were completely immersed into the liquid metal bath confirmed the strong agitation produced by gas evolution. Little variation in melting rate of pellets may be attributed to the difference in composition of the pellets. For 16-17

mm diameter pellets, the time required for complete dissolution in fully immersed condition in liquid metal bath was observed to be 83-90 seconds. These values can be comparable as it was also reported in the literatures [106, 109] that a typical dissolution time for a composite pellet into the slag layer (slag temperature 1773 K) in an open top crucible of induction furnace was in the order of 60 to 90 seconds.

6.2 Kinetics of Composite Pellets during Smelting

Kinetics in iron ore reduction deals with the rate at which iron oxides are converted to metallic iron by the removal of oxygen. The rate at which the ore is reduced influences the production rate of the process and determines its economic feasibility and competitiveness with other processes. The rate of reduction increases as the temperature increases. Smelting reduction of composite pellets (in liquid metal bath) involves solid, liquid and gas phases and hence the reactions are hetrogeneous. The movements of reactants and products at the interface are affected by several factors and in turn control the rate of reduction. A comprehensive review on kinetics of smelting reduction of composite pellets is discussed in Sections 2.2.8 and 2.2.9.

6.2.1 Results for dissolution of composite pellets in liquid metal bath

The experimental procedure for study of kinetics of smelting reduction of composite pellets is outlined in Section 4.6.3 and the variables and experimental conditions are listed in Table 4.14. The composition of composite pellets is given in Table 4.8. The result of dissolution of composite pellets in liquid metal bath at a temperature of 1723 ± 10 K is presented in Table 6.1.

(a) Degree of reduction for composite pellet in liquid metal bath

In present investigation, Eq. (3.81), as given below, is used to calculate the degree of reduction for composite pellets.

$$\alpha = \frac{400}{7} \times \left[\frac{f_{wl} - (f_{coal} \times f_{vm} \times f_{vr})}{(f_{ore} \times \rho_{ore} \times f_o)} \right] \quad \text{..... (3.81)}$$

Where, f_{wl} = Fractional weight loss = (weight loss of sample / initial weight of sample)

f_{coal} = Fraction of coal present in composite pellet

f_{vm} = Fraction of volatile matters present in coal

Table 6.1: Results for dissolution of composite pellets in liquid metal bath

Pellet Code*	Fe_{tot}/ C_{fix} Ratio	Time of Immers-ion (s)	Initial Wt. of Pellet, W_i(g)	Final Wt. of Pellet, W_f(g)	Difference in Weight, W_r (g)	Fractio-nal Wt. Loss, f_{wl}	Fracti-on of Reduc-tion, F	Rate of Reduc-tion, k (s^{-1})
ACP-1	2.50	10	5.4912	5.0080	0.4832	0.0880	0.1262	$1.26x10^{-2}$
		20	5.6786	4.7730	0.9056	0.1595	0.3684	$1.84x10^{-2}$
		30	5.6766	4.2929	1.3837	0.2438	0.6549	$2.18x10^{-2}$
		40	6.2677	4.3378	2.9299	0.3079	0.8725	$2.18x10^{-2}$
ACP-2	3.11	10	8.0324	7.3773	0.6551	0.0816	0.1205	$1.21x10^{-2}$
		20	9.1013	7.7120	1.3893	0.1526	0.3463	$1.73x10^{-2}$
		30	8.3539	6.3670	1.9864	0.2378	0.6170	$2.06x10^{-2}$
		40	6.9078	4.7966	2.1112	0.3056	0.8325	$2.08x10^{-2}$
ACP-3	3.50	10	6.7635	6.2366	0.5269	0.0779	0.1167	$1.17x10^{-2}$
		20	6.3240	5.3661	0.9579	0.1515	0.3433	$1.72x10^{-2}$
		30	6.1091	4.7242	1.3849	0.2267	0.5748	$1.92x10^{-2}$
		40	6.7826	4.8229	1.9597	0.2889	0.7664	$1.92x10^{-2}$
ACP-4	4.00	10	5.8016	5.3705	0.4311	0.0743	0.1133	$1.13x10^{-2}$
		20	7.0851	6.1862	0.8989	0.1269	0.3116	$1.56x10^{-2}$
		30	5.8723	4.6607	1.2116	0.2063	0.5063	$1.69x10^{-2}$
		40	5.6480	4.1454	1.5026	0.2660	0.6841	$1.71x10^{-2}$
BCP-1	2.50	10	4.6463	4.0630	0.5833	0.1255	0.1523	$1.52x10^{-2}$
		20	5.5113	4.3981	1.1132	0.2020	0.3991	$2.00x10^{-2}$
		30	6.5288	4.6235	1.9035	0.2918	0.6889	$2.30x10^{-2}$
		40	6.6292	4.2233	2.4059	0.3629	0.9184	$2.30x10^{-2}$
		50	6.3437	3.9207	2.4230	0.3820	0.9799	$1.96x10^{-2}$
BCP-2	3.11	10	5.9002	5.2100	0.6902	0.1170	0.1531	$1.53x10^{-2}$
		20	6.0034	4.8416	1.1618	0.1935	0.3858	$1.93x10^{-2}$
		30	6.9066	5.0198	1.8868	0.2732	0.6305	$2.10x10^{-2}$
		40	6.2336	4.0505	2.1831	0.3502	0.8626	$2.16x10^{-2}$
BCP-3	3.50	10	6.1449	5.4863	0.6586	0.1072	0.1367	$1.37x10^{-2}$
		20	6.0653	4.9742	1.0911	0.1799	0.3518	$1.76x10^{-2}$
		30	5.7407	4.2272	1.5135	0.2636	0.5995	$2.00x10^{-2}$
		40	5.7971	3.8948	1.9023	0.3281	0.7905	$1.98x10^{-2}$
		50	5.7867	3.7844	2.0023	0.3460	0.8434	$1.69x10^{-2}$
BCP-4	4.00	10	7.0719	6.4134	0.6659	0.0941	0.1127	$1.13x10^{-2}$
		20	7.2245	6.0167	1.2078	0.1672	0.3229	$1.61x10^{-2}$
		30	6.5681	4.9952	1.5729	0.2395	0.5308	$1.77x10^{-2}$
		40	6.1359	4.2276	1.9083	0.3110	0.7365	$1.84x10^{-2}$
		50	6.1448	4.0931	2.0517	0.3339	0.8023	$1.60x10^{-2}$

* ACP refers to the composite pellet made with coal from Jharia mines, Dhanbad and
* BCP refers to the composite pellet made with coal from Bhilai Steel Plant, Bhilai.

f_{vr} = Fraction of volatiles released during reduction at a particular temperature

f_{ore} = Fraction of ore present in composite pellet

ρ_{ore} = Purity of iron oxide (Fe_2O_3)

f_o = Fraction of oxygen present in Fe_2O_3

Calculation for the degree of reduction of composite pellet according to Eq. (3.81) is shown in Appendix 6A. The fraction of reduction (F) for composite pellets of different Fe_{tot}/C_{fix} ratios for 10, 20, 30, 40 and 50 seconds of immersion in liquid metal bath is presented in Table 6.1.

The amount of volatiles present in composite pellets selected for dissolution study was calculated and is shown in Appendix 6B. The weight loss of pellets immersed for 10 seconds in liquid metal bath was found higher than the amount of volatiles present in pellets. For 20, 30 and 40 seconds of immersion in liquid metal bath, the weight loss of pellets was found much higher than the amount of volatiles present in pellets. This indicates that the volatiles present in the pellet released within 10 seconds of the immersion of pellet into the liquid metal bath due to very high temperature.

Figure 6.1 shows the change in fraction of reduction of iron oxides with time for composite pellets immersed in liquid metal bath maintained at a temperature of 1723 ± 10 K. The time dependent reduction curve shows that the reduction at the initial stage proceeded relatively slower, at intermediate stage much faster, and at final stage again becomes slower (for BCP pellet). This is due to the release of volatile matters from the pellet as well as incubation period at the earlier stage. At intermediate stage, gases (mainly hydrogen) diffuse through the porous solid (due to release of volatiles from the composites), and finally the fraction of reduction decreases due to sintering and densification. It is reported [179] that up to 1073 K, the rate of reduction by H_2 is more rapid than by CO. Since the diffusivity of H_2 is about four times as fast as that of CO, the reduction rate at intermediate stage is faster than that of final stage. This is also reported by El-Geassy et al [46], and Sohn and Fruehan [49].

It was also observed that the fraction of reduction increases with decrease of Fe_{tot}/C_{fix} ratio. It is obvious that by decreasing Fe_{tot}/C_{fix} ratio, the carbon present in composite

pellet increases, i.e., more reductant present in pellet and hence more reduction takes place.

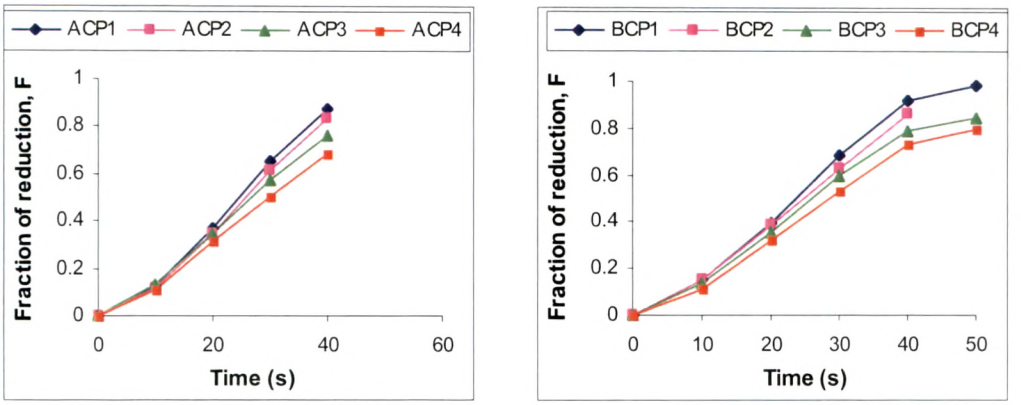

(a) (b)

Fig. 6.1: Reduction curve for (a) ACP and (b) BCP pellets in liquid metal bath.

For pellets of Fe_{tot}/C_{fix} ratio of 4.0 where carbon content is less in composite pellets, then at the final stage reduction the carbon from the melt diffuses towards pellet-melt interface and takes part in reaction $FeO + C_{melt} = Fe + CO$, which is a solid state reaction. This reaction is much slower than the gas-solid reaction. Further, at high temperatures, sintering of the iron particles takes place and structure becomes denser. So, the diffusivity of the gas as well as diffusion of carbon decreases which leads to decrease in rate of reduction as well as fraction of reduction. Similar results are reported in literature [46].

(b) Calculation for rate of reduction (k)

Rate of reduction (k) for composite pellets reduced in liquid metal bath is determined by dividing the fraction of reduction (F) by time (t) for which the pellet is immersed into the liquid metal bath.

$$k = \frac{F}{t} \qquad \text{.....(6.1)}$$

Where, k = rate of reduction, s^{-1}

F = fraction of reduction

t = time, s

For ACP1 pellet (Fe_{tot}/C_{fix} ratio of 2.50) immersed in liquid metal bath for 10 seconds, the rate of reduction (k) is calculated as follows:

$$k = \frac{0.1262}{10} = 1.262 \times 10^{-2}\ s^{-1} \qquad \text{.....(6.2)}$$

Similarly, the rate of reduction was calculated for other pellets of different Fe_{tot}/C_{fix} ratios and is shown in Table 6.1.

Figure 6.2 shows the rate of reduction curve. Initially, the reduction rate is very fast for both ACP and BCP pellets and later on the rate decreases with time. This is due to the release of volatiles at a time from the composite pellet, which causes rapid gas-solid reactions. Sintering and densification of product particles occur due to very high temperature, hence the rate of reduction decreases owing to poor diffusivity of gases and slower diffusion of carbon at final stage. This is also reported in the literatures [50, 180].

It is evident from Figure 6.3 that both the fraction of reduction (F) and rate of reduction (k) are higher for BCP pellets than that of ACP pellets. This is attributed to the high volatile content in coal from Bhilai Steel Plant (used in making BCP pellets). Sharma [176] reported that high volatiles in coal cause more porosity and leads to increased degree of reduction.

It is observed from Table 6.1 that for 30 to 40 seconds the change of rate of reduction (Δk) for ACP and BCP pellets comes to 0.0 to 0.02 $x10^{-2}$ s^{-1} and -0.02 to 0.07 $x10^{-2}$ s^{-1} respectively due to sintering and densification of the product particles. That is why both the rate of reduction and fraction of reduction decreased. These are also shown in SEM photographs 6.9 and 6.10.

For 30 seconds of pellet immersion in liquid melt, the change of rate of reduction (Δk) for

ACP1 - ACP4 pellet: $\Delta k = (2.18 - 1.69) \times 10^{-2} = 0.49 \times 10^{-2}\ s^{-1}$ and

BCP1 - BCP4 pellet: $\Delta k = (2.30 - 1.77) \times 10^{-2} = 0.53 \times 10^{-2}\ s^{-1}$

Difference in change of rate of reduction between ACP and BCP pellets = $0.04x10^{-2}$ s^{-1}

For 40 seconds of pellet immersion in liquid melt, the change of rate of reduction (Δk) for

ACP1 - ACP4 pellet: $\Delta k = (2.18 - 1.71) \times 10^{-2} = 0.47 \times 10^{-2}\ s^{-1}$ and

BCP1 - BCP4 pellet: $\Delta k = (2.30 - 1.84) \times 10^{-2} = 0.46 \times 10^{-2}\ s^{-1}$

Difference in change of rate of reduction between ACP and BCP pellets = $0.01x10^{-2}$ s^{-1}, which is negligible.

This means that up to 30 seconds, there are some effects of volatile matters on reduction but after 40 seconds, that effect is negligible. This is also reported by Wang et al [43], and Sohn and Fruehan [51].

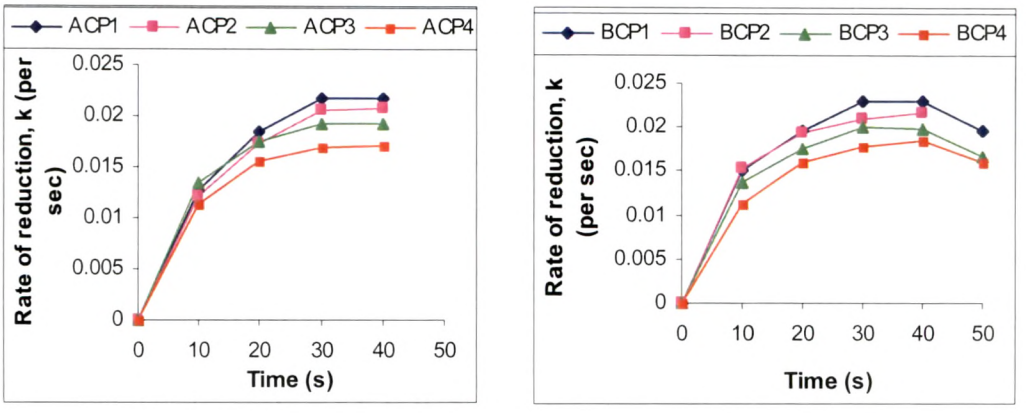

(a) (b)

Fig. 6.2: Rate of reduction for (a) ACP and (b) BCP pellets in liquid metal bath.

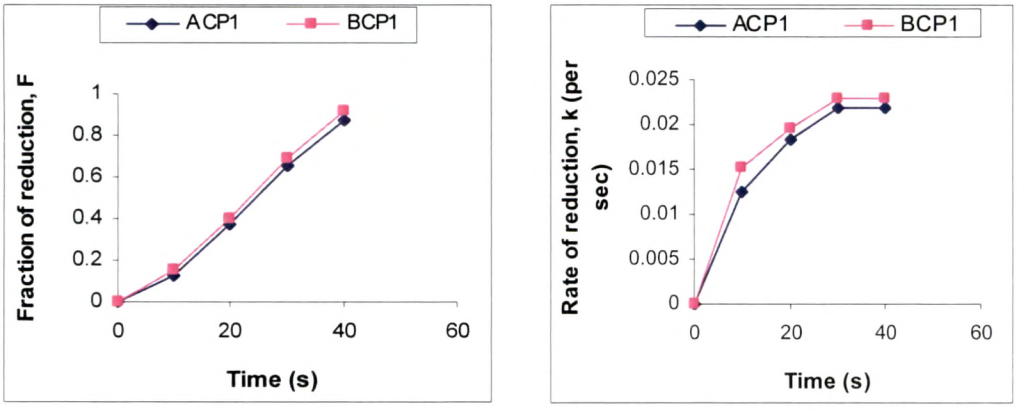

(a) (b)

Fig. 6.3: Comparison of reduction curves (a) fraction of reduction and (b) rate of reduction.

From Table 6.1, it may also be noted that:

i) The degree of reduction varied in the range of 68-87 pct for ACP (coal from Jharia mines) pellets for 40 seconds and 73-92 pct for BCP (coal from Bhilai steel plant) pellets for 40 seconds. The higher degree of reduction in BCP pellets is attributed to the high volatile matter content in Bhilai coal.

ii) For identical Fe_{tot}/C_{fix} ratio in ACP and BCP pellets, higher degree of reduction is obtained in BCP pellets, which is attributed to the high volatile matter content (i.e., more release of reducing gases H_2 and CO) in Bhilai coal.

iii) For BCP pellets immersed in liquid melt for 50 seconds, the degree of reduction varied in the range of 80-98 pct. This indicates that the reduction process continues even after 40 seconds.

6.3 Bulk Dissolution of Composite Pellets in Smelting Reduction and Iron Recovery

The experimental procedure for bulk dissolution of composite pellets and recovery of iron is outlined in Section 4.6.4 and the variables and experimental conditions are listed in Table 4.14. The composition of composite pellets is given in Table 4.8. The result of the melting of composite pellets is given in Table 6.2. According to the Eq. (4.8), calculation for iron yield of heat H1, where ACP1 pellets (Fe_{tot}/C_{fix} ratio = 2.50) were used, is shown in Appendix 6C.

Table 6.2: Results of composite pellet dissolution in induction furnace

- Argon gas flow rate: 1500 cc/min in all heats
- Temperature of the melt: 1723 ± 10 K
- Total time taken for heat (tap to tap time): 1 hr 15 min to 1 hr 30 min

Heat No.	Pellet Code	Fe_{tot}/C_{fix} Ratio	Scrap (input) (g)	Pellet (input) (g)	Metal (output) (g)	Iron Yield (pct)	Weight of slag (g)	Pellet dissolution period (min)
H1	ACP-1	2.50	3000	1000	3302	96.94	310	35
H2	ACP-2	3.11	3000	1000	3244	95.03	286	30
H3	ACP-3	3.50	3000	1000	3306	96.14	270	35
H4	ACP-4	4.00	3000	1000	3280	95.02	262	32
H5	BCP-1	2.50	3000	1000	3339	97.50	290	40
H6	BCP-2	3.11	3000	1000	3285	95.32	280	35
H7	BCP-3	3.50	3000	1000	3328	96.26	260	28
H8	BCP-4	4.00	3000	1000	3300	95.14	235	30

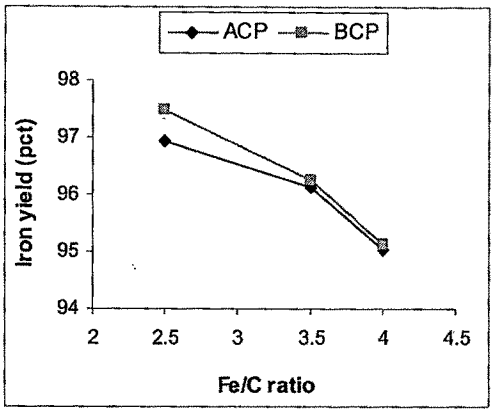

Fig. 6.4: Iron yield *vs* Fe/C ratio

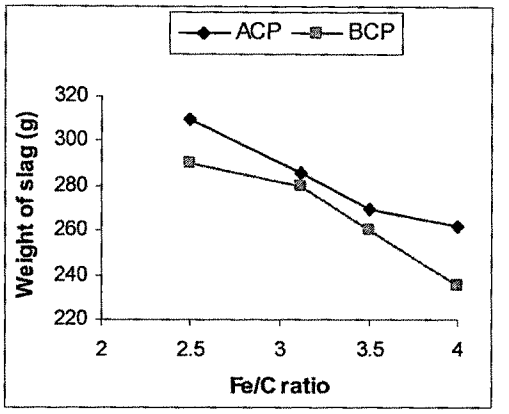

Fig. 6.5: Slag weight (experimental) *vs* Fe/C ratio

Figure 6.4 shows that with increase in Fe_{tot}/C_{fix} ratio the iron yield decreases. This is due to the lower carbon content in pellets which leads to incomplete reduction of iron oxides. From Figure 6.5, it is observed that with increase in Fe/C ratio the slag weight decreases. With increase in Fe/C ratio in composite pellet, the percentage of coal decreases and thereby the amount of ash content goes down. This leads to the decrease in slag weight. Further, it can be seen from Figure 6.5 that for the same Fe_{tot}/C_{fix} ratio of composite pellet, the quantity of slag produced is more with ACP pellets than that for BCP pellets. This is due to the higher ash content in coal from Jharia mines that is used for making ACP pellets.

6.3.1 Chemical Analysis

The chemical analyses of metal samples of castings were carried out using Optical Emission Spectrometer (OES) and LECO carbon-sulphur analyzer. The brief description of the instruments is given in Section 4.10. The results are presented in Table 6.3.

From Table 6.3, it can be seen that the silicon, manganese and sulphur content decreased in all heats due to their dilution in the melt. The tramp elements like chromium, nickel and copper (except molybdenum) decreased in all heats which is attributed to the dilution of these elements occurred during heat. As the content of tramp elements goes down, the quality of the product improves. Phosphorous content increased in all heats, which is attributed to the phosphorous coming from the iron ore of composite pellets charged into

the melt. With increase in Fe_{tot}/C_{fix} ratio, the iron ore content in composite pellets also increased and that is why phosphorous content in melt also increased (as shown in Table 4.8).

Table 6.3: Results of chemical analysis of samples

Heat No.	Sample No.*	Chemical composition (pct)								
		C	Mn	Si	S	P	Cr	Ni	Mo	Cu
H1	ACP1-I	1.79	0.09	0.27	0.114	0.27	0.21	0.19	0.04	0.18
H1	ACP1-F	1.95	0.03	0.20	0.113	0.30	0.19	0.19	0.04	0.16
H2	ACP2-I	1.68	0.19	0.58	0.081	0.25	1.19	1.52	0.04	1.53
H2	ACP2-F	1.49	0.12	0.40	0.072	0.28	1.09	1.31	0.04	1.23
H3	ACP 3-I	1.82	0.14	0.28	0.089	0.22	0.41	0.29	0.05	0.28
H3	ACP 3-F	1.69	0.11	0.23	0.083	0.26	0.38	0.26	0.05	0.23
H4	ACP 4-I	1.62	0.20	0.31	0.115	0.19	0.33	0.27	0.04	0.34
H4	ACP 4-F	1.33	0.14	0.27	0.102	0.23	0.27	0.23	0.04	0.27
H5	BCP1-I	1.96	0.09	0.34	0.100	0.15	0.18	0.22	0.04	0.16
H5	BCP1-F	2.05	0.04	0.28	0.086	0.19	0.15	0.19	0.04	0.14
H6	BCP2-I	2.57	0.21	0.52	0.072	0.19	1.26	1.42	0.04	0.47
H6	BCP2-F	2.46	0.13	0.40	0.069	0.22	1.17	1.27	0.04	0.40
H7	BCP3-I	2.29	0.05	0.23	0.108	0.38	0.19	0.22	0.04	0.17
H7	BCP3-F	2.16	0.03	0.17	0.105	0.42	0.15	0.17	0.04	0.14
H8	BCP4-I	1.86	0.16	0.29	0.114	0.21	0.23	0.21	0.04	0.18
H8	BCP4-F	1.21	0.11	0.23	0.099	0.23	0.20	0.16	0.04	0.15

* I : Initial sample collected before charging of composite pellets, and
F: Final sample collected after complete dissolution of composite pellets.

Figures 6.6 and 6.7 show the change of carbon and change of tramp elements [Σ (Cr + Ni + Mo + Cu)] from final to initial composition of the samples with Fe_{tot}/C_{fix} ratio respectively.

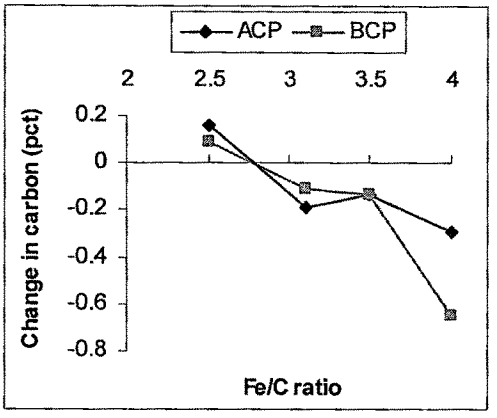

Fig. 6.6: Change in carbon *vs* Fe/C ratio

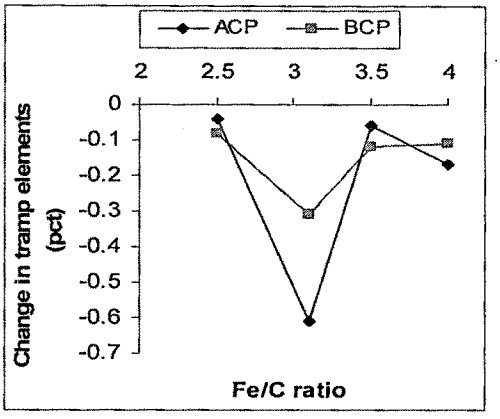

Fig. 6.7: Change in tramp elements *vs* Fe/C ratio

From Figure 6.6, it can be seen that the carbon content decreased in all heats except H1 and H5 where ACP1 and BCP1 pellets were used respectively. In both these pellets, the Fe_{tot}/C_{fix} ratio is low (2.5), which refers to more carbon than the stoichiometric (Fe_{tot}/C_{fix} = 3.11). The excess carbon in these composite pellets went into the melt resulting in carburization of the melt according to the reaction: $C_{(s)} = C_{(carburized)}$. Therefore, the carbon content of the product metal increased. In other heats, the carbon content is either equal to or less than the stoichiometric (theoretically required for complete reduction of iron oxides) and therefore, the carbon from the melt takes part into reduction of iron oxides. Further, the lower carbon content in product metal may be due to the dilution of carbon as more Fe is coming from reduction of iron oxides of composite pellets.

6.3.2 Mass balance

Mass Balance calculation for bulk dissolution of composite pellets in an induction furnace for heat H1, where ACP1 pellets (Fe_{tot}/C_{fix} ratio = 2.50) were used, is shown in Appendix 6D. Calculation is done according to the mathematical model developed for mass balance in Section 3.3.

6.4 X-ray Diffraction (XRD) Studies of Reduced Pellets

A brief description of the equipment and the procedure for X-ray diffraction (XRD) studies of reduced pellets is given in Section 4.8. The X-ray diffraction spectrum of reduced pellet, immersed in the liquid metal bath, is shown in Figure 6.8.

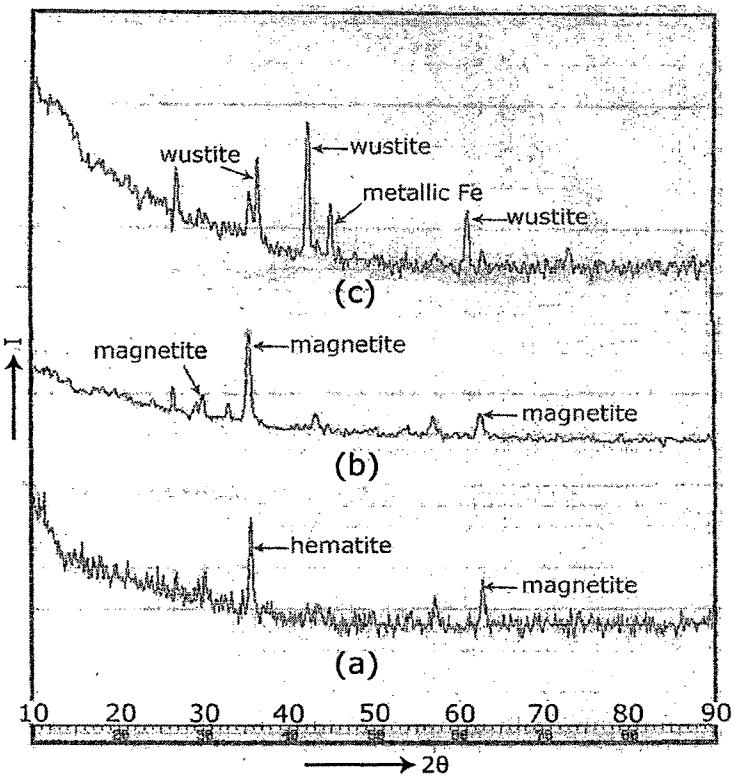

Fig. 6.8: X-ray diffraction spectra of reduced pellet (a) 20 s, (b) 30 s, and (c) 40 s.

The results of XRD studies are presented in Table 6.4. In case of sample reduced for 20 seconds, the major phase was hematite and minor phase was magnetite. For samples reduced for 30 seconds, the major phase observed was magnetite and minor phase was wustite. For samples reduced for 40 seconds in molten metal, the major phases were metallic iron and wustite. These observations can be explained by assuming that the reduction occurred topochemically, i.e., stage wise, e.g., $Fe_2O_3 \rightarrow Fe_3O_4 \rightarrow FeO \rightarrow Fe$. Other research workers [33, 39] observed similar types of results.

Table 6.4: Results of X-ray studies

Composite Pellet Code	Sample Code	Degree of Reduction (pct)	Phases Present
ACP2	ACP2 - 20	34.63	Fe_2O_3 and Fe_3O_4
	ACP2 - 30	61.70	Fe_3O_4
	ACP2 - 40	83.25	FeO and Fe

6.5 Scanning Electron Microscopic (SEM) Examination of Reduced Pellets

A brief description of the equipment and the procedure for scanning electron microscopic examination of reduced pellets is outlined in Section 4.6. Microstructural observation of several partially reduced samples, collected during smelting-reduction/dissolution of pellets in liquid metal bath, gave insight about the reduction of composite pellets. The SEM photomicrographs are helpful to understand the fundamentals of the reduction and process mechanism.

Photographs 6.1 to 6.10 present the morphological changes in pellet by observation with scanning electron microscope (SEM). The pellets were reduced in a molten metal bath maintained at 1723±10 K for 10, 20, 30, 40 and 50 seconds. Photograph 6.1 shows the outer surface structure of the composite pellet (prepared using Jharia coal) immersed in the liquid melt for 10 seconds. This photograph shows that some cracks are formed on the surface of the pellet. This may be due to the gas evolution that takes place during dissolution.

The photographs 6.2 and 6.3 are the fractured reduced surface immersed for 10 seconds in molten metal bath. Porous surface is seen in the photographs. This is due to the gas evolution that takes place during the dissolution process. Similar observation was made by Seaton et al [99]. The tunnel like appearance which clearly indicates the continuous gas evolution is shown in the photograph 6.4. This is due to the high volatile matters present in Bhilai coal.

Photographs 6.5 and 6.6 also show the porous surface and correspond to the pellets immersed in the liquid melt for 20 seconds. Photographs 6.7 and 6.8 correspond to the pellets immersed in the liquid melt for 30 seconds. In photograph 6.8, more porous and tunnel like structure is observed than that of photograph 6.7. This is attributed to the high volatile matters present in Bhilai coal. Similar results are reported by Seaton et al [99], and Yang et al [164]. In pellets immersed for 40 seconds in the melt, clusters of whiskers nucleated and grew on the FeO substrate as shown in photograph 6.9 and 6.10. Sintering and densification are also observed in these photographs.

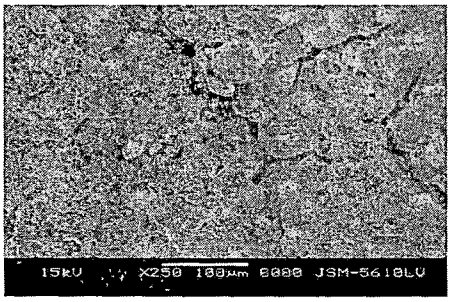

6.1: ACP2-10 s (outer surface), 250X

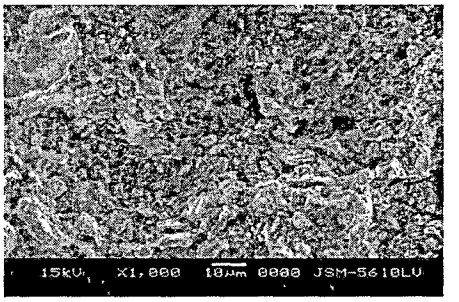

6.2: ACP2-10 s, 1000X

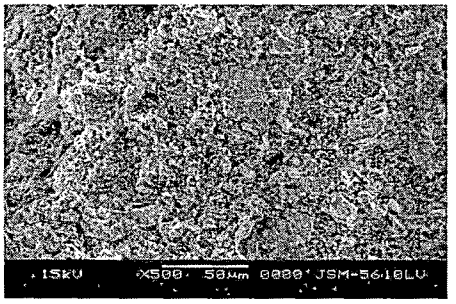

6.3: ACP2-10 s, 500X

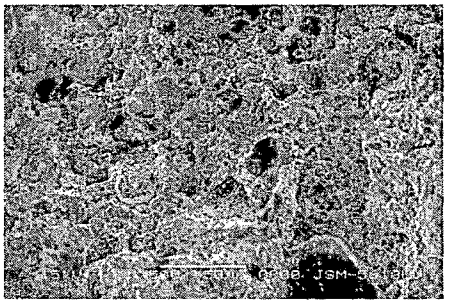

6.4: BCP2-10 s, 500X

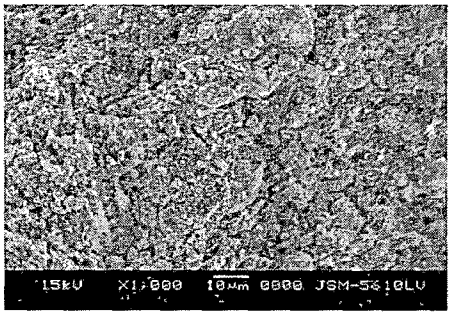

6.5: ACP2-20 s, 1000X

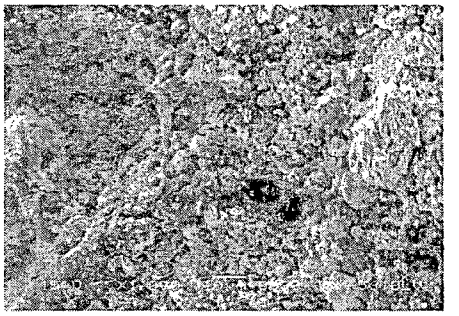

6.6: BCP2, 20 s, 1000X

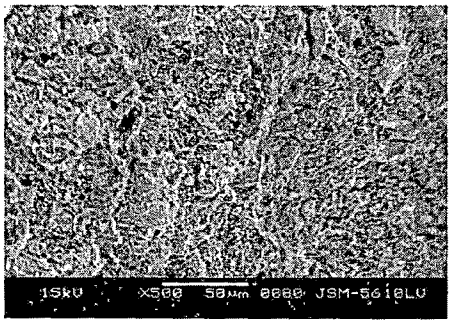

6.7: ACP2, 30 s, 500X

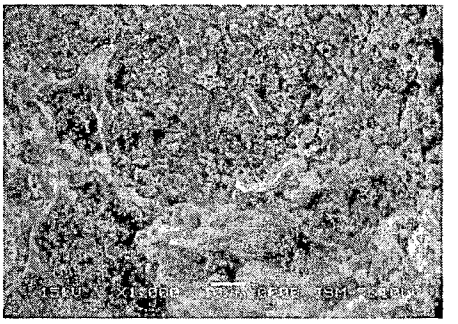

6.8: BCP2-30 s, 1000X

Photo 6.1 to 6.8: SEM photomicrographs of reduced pellets.

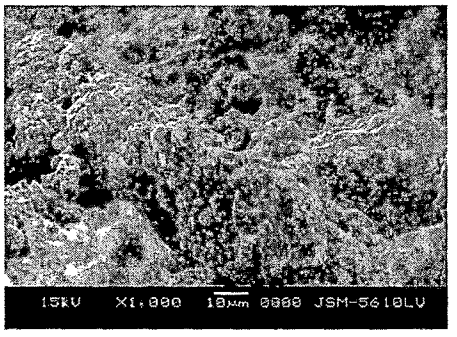

6.9: ACP2-40 sec, 1000X

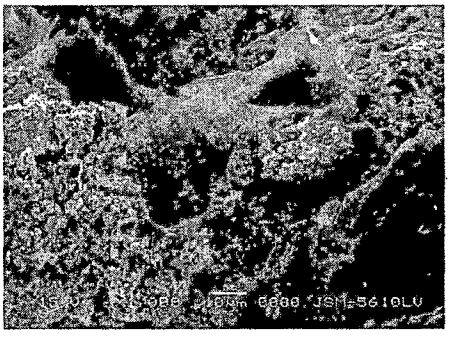

6.10: BCP1-40 s, 1000X

Photo 6.9 to 6.10: SEM photomicrographs of reduced pellets.

A brief summary of SEM observation of reduced pellets is presented in Table 6.5.

Table 6.5: Summary of SEM observation of reduced pellets

Photogr-aph No.	Pellet Code	Fe_{tot}/C_{fix} Ratio	Reduction Time (s)	Degree of Reduction (pct)	Morphology
6.1	ACP-2	3.11	10	12.05	cracks on the surface
6.2	ACP-2	3.11	10	12.05	porous surface
6.3	ACP-2	3.11	10	12.05	porous surface with less tunnel like structure
6.4	BCP-2	3.11	10	15.31	porous surface with more tunnel like structure
6.5	ACP-2	3.11	20	34.63	porous surface
6.6	BCP-2	3.11	20	38.58	porous surface with few tunnel like structure
6.7	ACP-2	3.11	30	61.70	highly porous and tunnel like structure
6.8	BCP-2	3.11	30	63.05	
6.9	ACP-2	3.11	40	83.25	sintered structure with clusters of whiskers
6.10	BCP-1	2.50	40	91.84	